**Supramolecular Chemistry**
Publication details, including instructions for authors and subscription information:
http://www.informaworld.com/smpp/title~content=t713649759

# New Exo-Functional Cyclophane Hosts. Synthesis and Crystal Structures of Inclusion Compounds

Romy Golbs[a]; Wilhelm Seichter[a]; Edwin Weber[a]; Ingeborg Csöregh[b]
[a] Institut für Organische Chemie der Technischen Universität Bergakademie Freiberg, Freiberg/Sachsen, Germany [b] Department of Structural Chemistry, Arrhenius Laboratory, Stockholm University, Stockholm, Sweden

**To cite this Article** Golbs, Romy , Seichter, Wilhelm , Weber, Edwin and Csöregh, Ingeborg(2006) 'New Exo-Functional Cyclophane Hosts. Synthesis and Crystal Structures of Inclusion Compounds', Supramolecular Chemistry, 18: 4, 333 — 348
**To link to this Article: DOI:** 10.1080/10610270600589816
**URL:** http://dx.doi.org/10.1080/10610270600589816

*Supramolecular Chemistry*, June 2006 Vol. 18 (4), pp. 333–348



# New Exo-Functional Cyclophane Hosts. Synthesis and Crystal Structures of Inclusion Compounds

ROMY GOLBS[a], WILHELM SEICHTER[a], EDWIN WEBER[a,*] and INGEBORG CSÖREGH[b]

[a]*Institut für Organische Chemie der Technischen Universität Bergakademie Freiberg, Leipziger Street 29, Freiberg/Sachsen D-09596, Germany;*
[b]*Department of Structural Chemistry, Arrhenius Laboratory, Stockholm University, Stockholm S-10691, Sweden*

*Received (in Southampton, UK) 10 December 2005; Accepted 21 January 2006*



**The new cyclophane type host compounds 1–3, containing rigid aromatic units and two exo-topic carboxylic acid functions, have been synthesized. Crystalline solvent inclusions, involving the dicarboxylic acid hosts and their corresponding ester intermediates 6 (a–c), namely 1·DMSO (1:4), 2·pyridine (1:3), 3·pyridine (1:4), 6a·pyridine (1:2) and 6a·benzene (1:2), have been prepared and studied using X-ray diffraction on single-crystals. Moreover, X-ray structure analyses of the solvent-free crystals of the 6 (a, b) intermediates were also carried out for comparison. Co-crystals of the carboxylic hosts 1–3 contained H-bonded 1:2 host-guest associates as building blocks, together with additional space-filling guests, whereas only loosely bounded space-filling solvent molecules were found in the two solid inclusion compounds of the 6a cyclophane ester host. In addition to the mentioned conventional H-bond interactions between carboxylic hosts and their guests, the crystal structures proved to be held together by relatively weak C–H···O bonds besides the ordinary van der Waals' interactions. Packing relations, and the effects of structural variations, guest molecules and anisotropic packing forces on the conformation of the semi-rigid cylcophane ring have been discussed and compared in seven crystal structures.**

*Keywords*: Cyclophane hosts; Organic guests; Crystalline inclusion compounds; Supramolecular interactions; X-ray crystal structure determinations

## INTRODUCTION

Macrocyclic host compounds [1] are of continuing interest in supramolecular chemistry [2,3]. Apart from crown ethers and cryptands [4,5], cyclophane-type macrocycles [6] are important exponents of this compound class [7]. They feature a rather rigid host framework arising from the assembly of aromatic groups, which leads to well-defined cavity structures [8,9]. Angular diphenyl methane or analogously shaped building blocks have been used most frequently for this purpose [10–13]. Corresponding cyclophanes are versatile host compounds represented by a great many structures in which the guest is either entrapped in the cyclophane cavity or is sandwiched between the host molecules in the crystal lattice [6,9–13].

In order to improve the endo mode of host behaviour, convergent functional sites such as carbocyclic groups have been incorporated into the cyclophane scaffold [14–16]. On the other hand, the construction of highly organized and complex structures using supramolecular synthon strategy [17] is an exciting emergent subfield of supramolecular chemistry [18]. In this connection, exo-topic instead of endo-topic functional groups are desirable, giving rise to a potential excess of extended self-assembling oligomeric supramolecular structures [19] interspersed with macrocyclic holes, which may serve as a useful porous matrix for including guest molecules [20]. This prompted us to turn the carboxylic groups of previously described endo-receptor cyclophanes [14–16] from the inside to the outside, or from endo to exo orientation, thus producing exo-functional cyclophane receptors **1**–**3** (Scheme 1).

In this article we present the experimental details of the synthesis of **1**–**3** and report the X-ray crystal structures of selected inclusion compounds formed from the macrocyclic dicarboxylic acids **1**–**3** and their intermediate ester derivatives **6a**–**6c**.

## RESULTS AND DISCUSSION

### Synthesis

The synthesis of the present exo-functional host compounds (**1**–**3**), based on 3,5-disubstituted benzoic

*Corresponding author. Fax: + 49-37-31-39-31-70. E-mail: edwin.weber@chemie.tu-freiberg.de

ISSN 1061-0278 print/ISSN 1029-0478 online © 2006 Taylor & Francis
DOI: 10.1080/10610270600589816

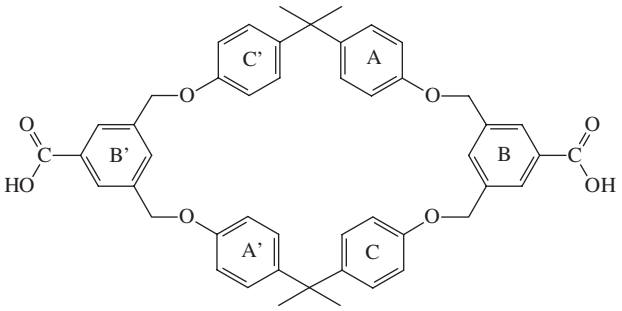


**1**

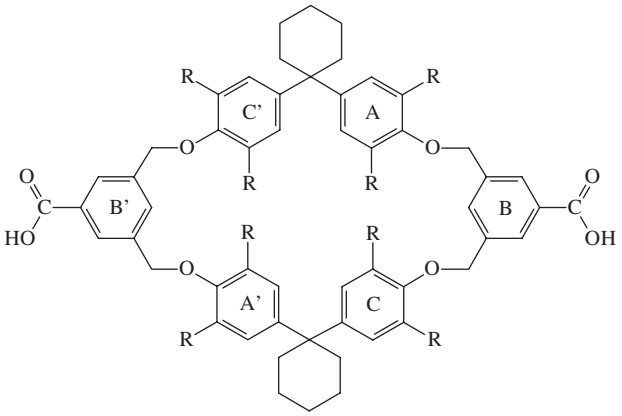


**2** R = H
**3** R = $CH_3$

SCHEME 1 Host macrocycles studied in this paper.



acid and a building block analogous to diphenyl methane, follows a design strategy (Scheme 2) that has previously proved to be successful in the formation of new endo-functional cyclophane receptors [14–16]. The key step of the synthesis is the ring closure reaction of bis-benzylic dibromide **4** [21] with diphenols **5a–c** [22,23] to give the macrocyclic esters **6a–c**. High dilution conditions [24,25] and cesium carbonate as the base [26] were used for this process. Hydrolysis of the esters **6a–c** was performed with cesium hydroxide in *n*-butanol [16] followed by addition of aqueous hydrochloric acid to yield the macrocyclic diacids **1–3**.

## Structural Study

X-ray diffraction analyses of seven crystal structures, including inclusion complexes and unsolvated species of the exo-carboxylic hosts and intermediate ester derivatives, namely **1**·DMSO (1:4), **2**·pyridine (1:3), **3**·pyridine (1:4), **6a**·pyridine (1:2), **6a**·benzene (1:2), **6a** and **6b**, have been carried out. The selection of the compounds was mainly directed by the ability of the macrocyclic species to form crystals suitable for single-crystal X-ray diffraction study. Basic crystallographic information for the crystal structures is presented in Table I. Figures 1–10 show the molecular and packing illustrations of the respective compounds. Selected conformational parameters of the macrocyclic rings of the host molecules, and relevant intermolecular contacts are presented in Tables II and III, respectively.

### *Inclusion Compounds of the Dicarboxylic Acid Functional Cyclophane Hosts*

The crystal structures of three solvated, slightly different cyclophane dicarboxylic acid hosts **1–3** (Scheme 1), have been investigated. The three solid inclusion compounds, namely **1**·DMSO (1:4), **2**·pyridine (1:3), and **3**·pyridine (1:4) (Fig. 1a–c), exhibit similarities as well as distinct differences. The single crystals were grown from polar solvents, and the respective solvent molecules were found to be included in the crystals through host–guest hydrogen bond interaction in all three cases. Moreover, all three co-crystals also contain additional guests, located either inside the macrocycle (e.g. in **1**·DMSO (1:4) and **2**·pyridine (1:3)), or between the H-bonded 1:2 host–guest units (such as in **3**·pyridine (1:4)). The guest molecules (both the H-bonded and the space-filling ones) were found to be more or less disordered at room temperature, exhibiting in most cases not only dynamic but also static disorder (as indicated by the displacement parameters and the partial site occupation factors of the guest atoms, respectively). The only exception is the H-bonded pyridine molecule (P1) in the **2**·pyridine (1:3) complex (Fig. 1b), for which no static, and only moderate dynamic disorder was detected. At the same time, the space-filling guest (P2) in the same complex is located on a crystallographic inversion centre, and since the pyridine ring has no molecular inversion symmetry, at least two centrosymmetrically related, overlapping disorder sites must be assumed for that latter guest in order to satisfy the crystal symmetry requirements.

Crystallization of host **1** from dimethyl sulphoxide yielded triclinic co-crystals with the host:guest stoichiometry 1:4 (Fig. 1a). In addition to the disordered guest molecules, also one of the oxygens of the macrocyclic host, O(16), proved to occupy two possible disorder sites in this structure. As strong acceptors, two of the guest molecules (molecules 1 and 2, Fig. 1(a)) are linked *via* O–H···O hydrogen bonds (Table III) to the carboxyl groups of the host, as expected [27]. The two remaining symmetry-independent DMSO molecules (guest molecules 3 and 4, Fig. 1(a)) are included in the crystal through weaker interactions (see below). These latter guests seem to stabilize the packing arrangement by filling up the voids, thus increasing the packing density.

The cyclophane ring has molecular inversion symmetry (cf. Scheme 1). Nevertheless, host **1** exhibits an asymmetric curved conformation in its DMSO inclusion crystal (Table II), in all probability

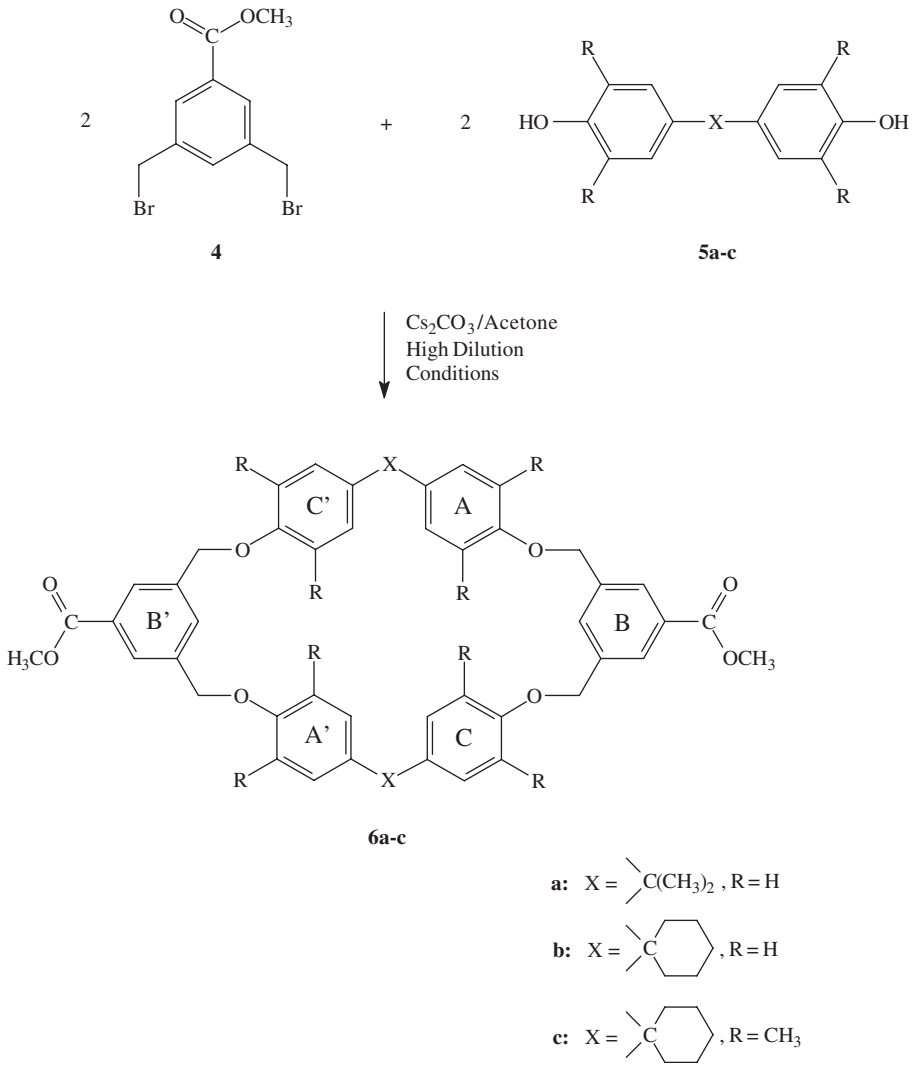


SCHEME 2 Synthesis of the host macrocycles.

due to directional intermolecular interactions and anisotropic packing forces in the crystal. The most remarkable conformational anomaly is indicated by the torsion angles $\tau_1$(C(14)–C(16)–O(16)–C(17)) = 103.0(5) and $\tau_2$(C(36)–C(38)–O(38)–C(39)) = 145.1(3)°, corresponding to the lower and upper limits of the energetically less favourable *anticlinal* conformation. The asymmetry of the macrocyclic ring conformation is also well manifested by the dihedral angles calculated for selected pairs of phenyl ring planes within the cyclophane ring **1** (Table II). Accordingly, worth noting are the considerable differences between related interplanar angles, calculated either for the A/B and A′/B′ pairs of ring planes or for the B/C and B′/C′ ones (Scheme 1, Table II). Moreover, the dihedral angles formed by the aromatic rings with opposite locations within the macrocycle, i.e. rings A/A′, B/B′ and C/C′ (Table II), indicate drastic deviation from coplanarity for each pair of them. At the same time, the dihedral angles between the aromatic ring planes of the bis-phenol moieties (i.e. between rings A/C′ and A′/C, Table II) nearly agree with each other, and compare also with the corresponding angles in the related hosts **2**, **3**, **6a** and **6b** (Table II), indicating approximately perpendicular arrangement for the bis-phenol phenyl ring planes in all studied cyclophanes.

The packing illustration (Fig. 2) shows a stacking arrangement, consisting of parallel columns along the crystallographic *a*-axis, with endless channels inside. Inspection of the intermolecular contact distances indicates a number of C–H···O interactions between the molecules (Table III). The included DMSO solvent molecules take active part in these interactions, not only as proton acceptors but also as proton donors through their weakly acidic methyl H atoms [28,29]. The space-filling guests, i.e. DMSO molecules 3 and 4 (Fig. 1(a)), form infinite C–H···O bonded strands extending along the host channels (Fig. 2). The mode of interaction within these strands leads to a uniform alignment of the

TABLE I Crystal data and selected details of data reduction and structure refinement calculations of the studied compounds

| Compound | **1**·DMSO (1:4) | **2**·Pyridine (1:3) | **3**·Pyridine (1:4) | **6a**·Pyridine (1:2) | **6a**·Benzene (1:2) | **6a**·(unsolvated) | **6b**·(unsolvated) |
|---|---|---|---|---|---|---|---|
| Empirical formula | $C_{48}H_{44}O_8$·4 ($C_2H_6SO$) | 0.5($C_{54}H_{52}O_8$)·1.5 ($C_5H_5N$) | 0.5($C_{62}H_{68}O_8$)·2 ($C_5H_5N$) | 2 ($C_{50}H_{48}O_8$)·4 ($C_5H_5N$) | 0.5[$C_{50}H_{48}O_8$·2·($C_6H_6$)] | 0.5($C_{50}H_{48}O_8$) | 0.5($C_{56}H_{56}O_8$) |
| Formula weight | 1061.34 | 533.13 | 628.78 | 1870.17 | 466.55 | 388.44 | 428.5.0 |
| Crystal system | Triclinic | Monoclinic | Monoclinic | Monoclinic | Monoclinic | Triclinic | Monoclinic |
| Space group | $P-1$ | $P2_1/a$ | $P2_1/n$ | $P2_1$ | $P2_1/c$ | $P-1$ | $P2_1/n$ |
| Unit cell dimensions: | | | | | | | |
| $a$ (Å) | 10.154(2) | 17.905(2) | 10.1769(6) | 10.431(1) | 10.3279(8) | 6.6339(3) | 10.532(1) |
| $b$ (Å) | 14.816(2) | 8.848(1) | 18.1622(8) | 29.226(3) | 29.102(2) | 11.7622(6) | 8.524(1) |
| $c$ (Å) | 20.337(2) | 17.996(2) | 19.385(1) | 16.114(2) | 8.1914(7) | 12.9899(8) | 25.240 (2) |
| $\alpha$ (°) | 100.67(2) | 90.0 | 90.0 | 90.0 | 90.0 | 98.788(3) | 90.0 |
| $\beta$ (°) | 95.66(2) | 95.572(13) | 92.535(5) | 94.66(1) | 97.496(4) | 98.587(3) | 98.78 (1) |
| $\gamma$ (°) | 106.32(2) | 90.0 | 90.0 | 90.0 | 90.0 | 91.694(3) | 90.0 |
| $V$ (Å$^3$) | 2848.6(7) | 2837.5(6) | 3579.5(3) | 4896.2(9) | 2441.0(3) | 989.04(9) | 2239.4(4) |
| $Z$ | 2 | 4 | 4 | 2 | 4 | 2 | 4 |
| $F$(000) | 1128 | 1132 | 1344 | 1984 | 992 | 412 | 912 |
| Radiation/$\lambda$ (Å) | Mo$K\alpha$/0.71073 | Mo$K\alpha$/0.71073 | Mo$K\alpha$/0.71073 | Mo$K\alpha$/0.71073 | Mo$K\alpha$/0.71073 | Mo$K\alpha$/0.71073 | Mo$K\alpha$/0.71073 |
| $D_c$ (Mg m$^{-3}$) | 1.237 | 1.248 | 1.167 | 1.269 | 1.270 | 1.304 | 1.271 |
| $\mu$ (mm$^{-1}$) | 0.225 | 0.081 | 0.075 | 0.084 | 0.083 | 0.087 | 0.084 |
| Data collection: | | | | | | | |
| Temperature (K) | 298(2) | 298(2) | 298 | 173(2) | 173(2) | 173(2) | 293(2) |
| No. of collected reflections within the $\theta$-limit (°) | 22603<br>2.0–26.0 | 20867<br>2.2–25.9 | 28597<br>2.3–26.0 | 33937<br>2.1–26.0 | 60572<br>2.1–31.0 | 23789<br>2.2–30.4 | 16693<br>2.2–25.9 |
| Index ranges, min/max $h$, $k$, $l$ | −12/12, −18/18, −24/24 | −21/21, −10/10, −22/22 | −12/12, −21/22, −23/23 | −12/11, −35/35, −19/19 | −13/14, −41/41, −11/11 | −7/9, −16/15, −18/18 | −12/12, −10/10, −30/30 |
| No. of unique reflections | 9837 | 5473 | 6587 | 16509 | 7731 | 5799 | 4305 |
| $R_{int}$ | 0.045 | 0.152 | 0.135 | 0.049 | 0.034 | 0.047 | 0.058 |
| Refinement calculation:[a] | | | | | | | |
| No. of refined parameters | 788 | 395 | 458 | 1370 | 349 | 289 | 318 |
| $R(=\sum\|\Delta F\|/\sum\|F_o\|)$ for $F$ with $I > 2\sigma(I)$ | 0.073 | 0.053 | 0.065 | 0.048 | 0.043 | 0.049 | 0.041 |
| No. of $F$ values with $I > 2\sigma(I)$ | 6058 | 2415 | 2004 | 12211 | 6066 | 3554 | 3038 |
| $WR$ for all unique $F^2$ values | 0.216 | 0.116 | 0.195 | 0.111 | 0.115 | 0.125 | 0.103 |
| Weighting expression for $w$[b] | $[\sigma^2(F_o^2) + (0.1230P)^2 + 0.0035P]^{-1}$ | $[\sigma^2(F_o^2) + (0.0340P)^2 + 0.0000P]^{-1}$ | $[\sigma^2(F_o^2) + (0.0818P)^2 + 0.0000P]^{-1}$ | $[\sigma^2(F_o^2) + (0.0575P)^2 + 0.000P]^{-1}$ | $[\sigma^2(F_o^2) + (0.0578P)^2 + 0.586P]^{-1}$ | $[\sigma^2(F_o^2) + (0.0500P)^2 + 0.070P]^{-1}$ | $[\sigma^2(F_o^2) + (0.0560P)^2 + 0.000P]^{-1}$ |
| $S$ (= Goodness of fit on $F^2$) | 1.113 | 0.866 | 0.839 | 1.013 | 1.057 | 1.069 | 1.034 |
| Final $\Delta\rho_{max}/\Delta\rho_{min}$ (e$^-$Å$^{-3}$) | 0.40/−0.32 | 0.16/−0.17 | 0.14/−0.14 | 0.21/−0.21 | 0.41/−0.26 | 0.29/−0.22 | 0.16/−0.14 |

[a] Full-matrix least-squares calculation on $F^2$, following *SHELXL-97* [45]. [b] $P = (F_o^2 + 2F_c^2)/3$ (cf. *SHELXL-97*, [45]).

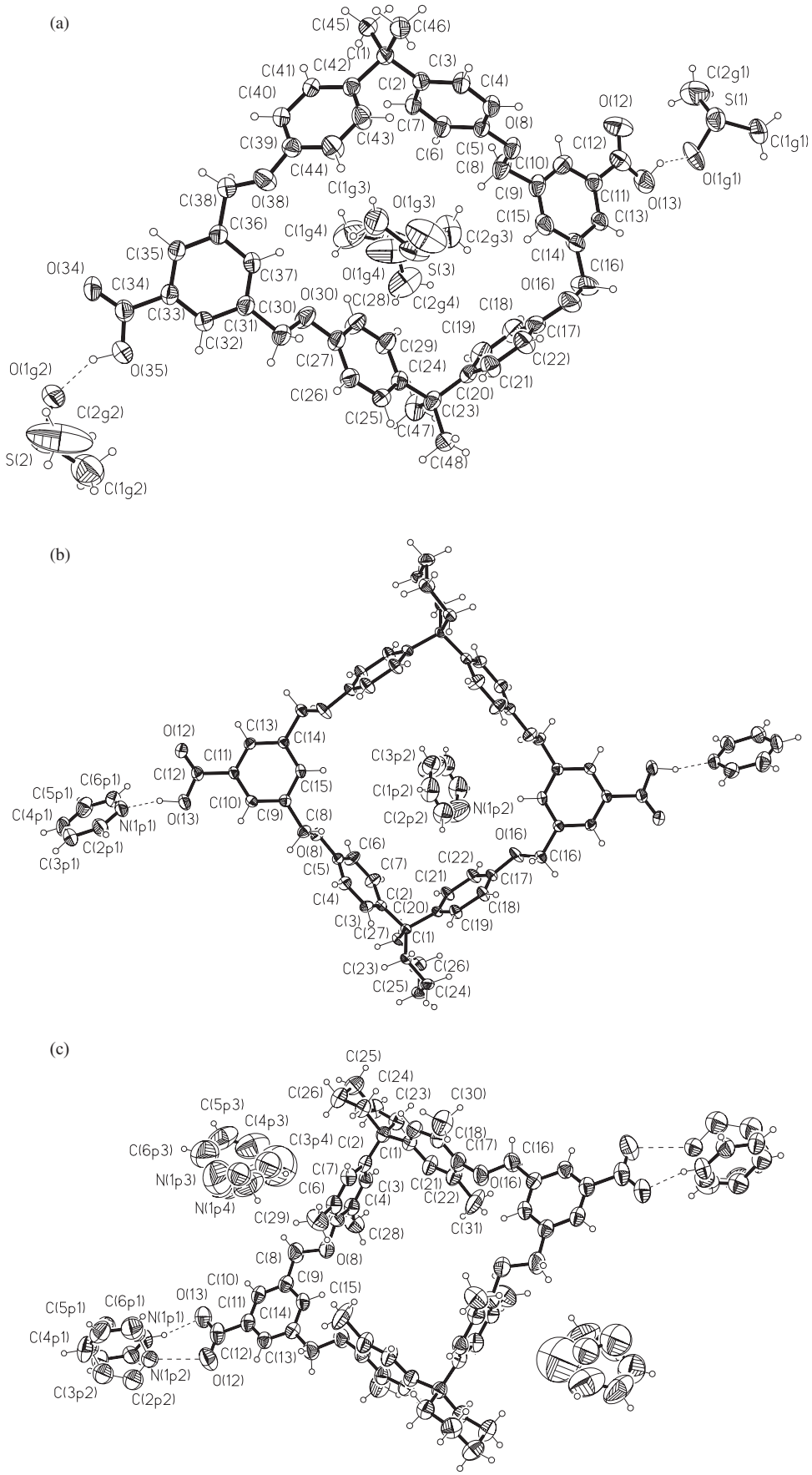


FIGURE 1 Perspective views of the stoichiometric units of the solid inclusion compounds **1**·DMSO (1:4) (a), **2**·pyridine (1:3) (b) and **3**·pyridine (1:4) (c). Atomic displacement ellipsoids of the non-hydrogen atoms are drawn at 30% probability level, and the unique positions are labelled. Solid and dashed lines indicate covalent and hydrogen bonds, respectively.

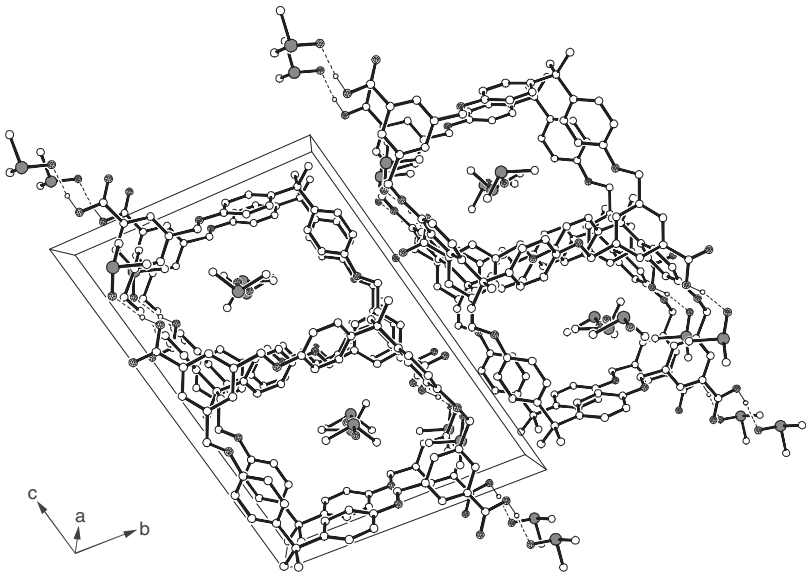


FIGURE 2 Packing illustration of **1** · DMSO (1:4) co-crystal. One position of each pair of disorder sites of the guest molecules together with the H atom positions are omitted for clarity. H bonds are displayed as dashed lines.



molecular dipoles. However, due to the inversion symmetry of the co-crystal, the strands in neighbouring host channels run in opposite directions, hence yielding zero total dipole moment for the complex crystal. Besides the van der Waals forces, the stacks of molecules are held together by weak but directional C–H···O interactions [29] (Table III).

Crystallization of cyclophane hosts **2** and **3** from pyridine yielded monoclinic co-crystals with 1:3 and 1:4 host:guest ratios, respectively (Fig. 1(b)–(c)). The stoichiometric units have inversion symmetry in both crystals, hence only one half of the host macrocycle together with $1\frac{1}{2}$ and 2 guest pyridines, respectively, form the unique parts of the structures. One unique pyridine guest is hydrogen bonded to the host carboxy function, and thus, by virtue of the inversion symmetry, 1:2 host–guest associates are created in both complexes. However, interestingly enough, the host–guest interaction modes seem to be different. The host carboxy function is the proton donor in the H-bond interaction to the guest in the **2**·pyridine (1:3) complex, just as in **1**·DMSO (1:4), but not in the **3**·pyridine (1:4) co-crystal. Unlike in molecules **1** and **2**, the two independent carboxy C–O distances in host **3** are practically equal (C(12)–O(12) = 1.242(6) and C(12)–O(13) = 1.245(6) Å), hence clearly indicating equal bond order for the two C–O bonds and delocalization of the π electrons within each carboxy group. At the same time, the pyridine guest, with potential for H-bond interaction with the host carboxy function, has been found to occupy two disorder sites (P1 and P2, Fig. 1c), in which the pyridine N positions (N(1P1) and N(1P2), Table III) are strategically located for H-bond interactions with the host O(13) and O(12) atoms, respectively. Moreover, despite the extended disorder involving both the donor and the acceptor groups, an acceptable H disorder site could be realized near to the major pyridine site (N(1P1)). Accordingly, the results of the X-ray diffraction study suggest that, in the present complex of host **3,** a protonated pyridine nitrogen is the proton donor and one or the other of the two oxygens in the deprotonated host $COO^-$ group is the acceptor in the host–guest H-bond interaction.

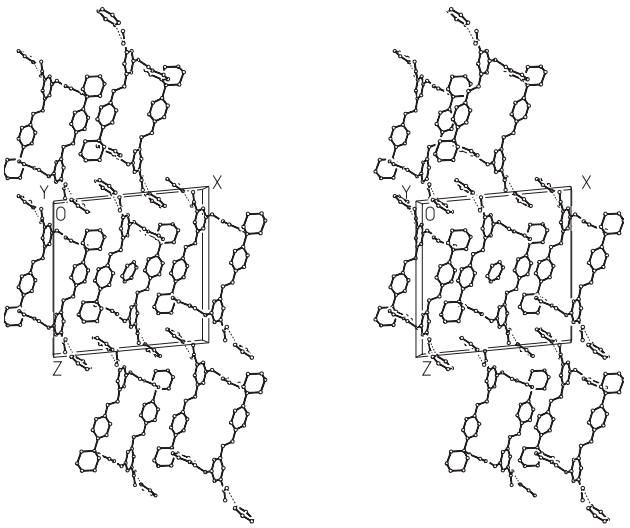


FIGURE 3 Stereo packing illustration of **2**·pyridine (1:3) complex. H atoms are omitted for clarity. Dashed lines indicate H bond interaction.

The molecular and crystallographic inversion symmetries of the cyclophane ring coincide in both pyridine inclusion compounds (**2**·pyridine (1:3) and **3**·pyridine (1:4)). In spite of the dimethyl substitution on the phenyl rings of the bis-phenol moieties in host **3**, the corresponding dihedral angles between

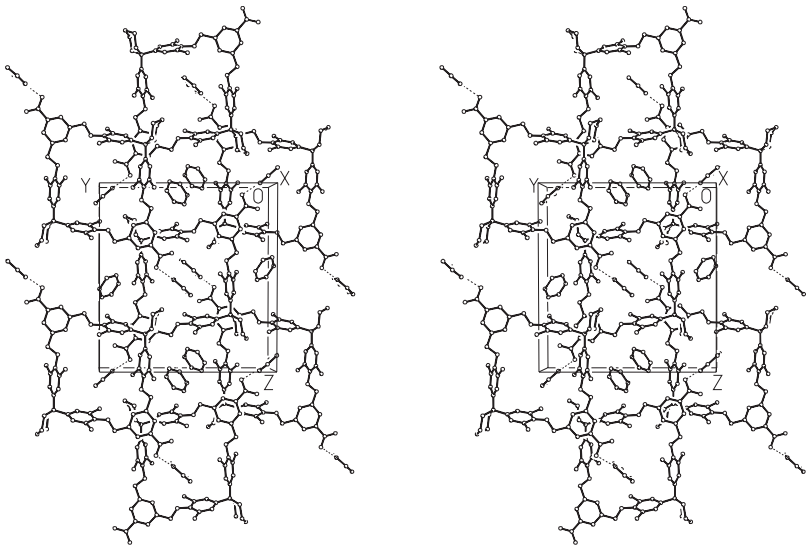


FIGURE 4 Stereo packing illustration of **3**·pyridine (1:4) inclusion crystal. H atoms are omitted for clarity. Dashed lines indicate H bond interactions.



selected phenyl ring planes (Table II) agree well with each other in the two molecules (**2** and **3**), suggesting similar macrocyclic ring conformations for them. The τ values for the $C(sp^2)$-$C(sp^3)$–O–$C(sp^2)$ sequences indicate the more relaxed *anti-periplanar* conformations for the connected phenyl rings in both molecules (**2** and **3**). Nevertheless, the tilt angle between the functionalized B ring and the attached –COO group, and also some of the ring torsion angles seem to be soft parameters, because they may differ significantly in these two cyclophanes (Table II).

Disregarding the host–guest hydrogen bonds mentioned above, inspection of the intermolecular connections in the crystals of these pyridine inclusion compounds suggests only weak interaction forces. Most of the observed approaches involve an oxygen atom on the one hand, and a carbon-bonded hydrogen on the other. However, only two such connections are listed in Table III for **2**·pyridine (1:3), and none for the **3**·pyridine (1:4) complex, because all the other contact distances are either relatively long (H···O ≈ 3.0 Å), or in case of shorter distances, the C–H···O angle is very unfavourable (C–H···O < 120°). Therefore, although the observed approaches clearly indicate an electrostatically favourable packing arrangement for both co-crystals (i.e. **2**·pyridine (1:3) and **3**·pyridine (1:4)) (Figs. 3 and 4), they do not prove the presence of directional C–H···O bonds for certain. Worth mentioning is that the packing illustration of the **2**·pyridine (1:3) complex (Fig. 3) gives an indication of possible edge-to-face interactions [30,31] between the A rings of the macrocycles related by the symmetry operation $-x + 0.5,\ y \pm 0.5,\ -z + 1$. However, the C···π/H···π distances (C···π > 4.05 and H···π > 3.36 Å) are too long to verify an attractive interaction of this type [30,31]. Considering the inclusion of the space-filling guests, the shortest host–guest contact distance involving guest P2, located within the host **2** macrocycle, is $C(2P2)\cdots O(8)_{0.5-x,\ -\ 0.5\ +\ y,\ 1\ -\ z} = 3.666(5)$, and those involving the guest on the P3/P4 disorder sites, outside the host **3** cavity, are $C(5P3)\cdots C(22)_{x+0.5,\ -\ y\ +\ 1.5,\ z\ -\ 0.5} = 3.49(1)$ and $C(4P4)\cdots C(16)_{x+0.5,\ -\ y\ +\ 1.5,\ z\ -\ 0.5} = 3.52(3)$ Å, respectively. Accordingly, although the space filling pyridines have different locations with respect to the macrocyclic hosts **2** and **3**, they seem to be included with the same function, namely to stabilize the crystal structure by increasing the packing density.

### *Inclusion Compounds of the Diester Substituted Cyclophane Hosts*

In order to grow crystals of the diester **6a** (Scheme 2) for single-crystal X-ray diffraction study, solvents with various polarity were tested. The structures of three of the yielded crystalline compounds have been analyzed, namely the solvent-free crystal of **6a** (crystallized from mesitylene solvent), and two inclusion compounds containing solvent molecules as guests, such as the polar pyridine in **6a**·pyridine (1:2) (Fig. 5a) and the non-polar benzene in **6a**·benzene (1:2) (Fig. 5b). The two inclusion crystals have monoclinic unit cells with the same 1:2 host:guest stoichiometry. One of the guests is located inside the host cavity, whereas the other resides in between the macrocyclic units in both cases. Despite these similarities, the realized packing arrangements in the two inclusion crystals of **6a** differ in many respects.

In the case of the **6a**·pyridine (1:2) co-crystal, the X-ray diffraction experiment indicated a monoclinic unit cell (Table I), containing four stoichiometric

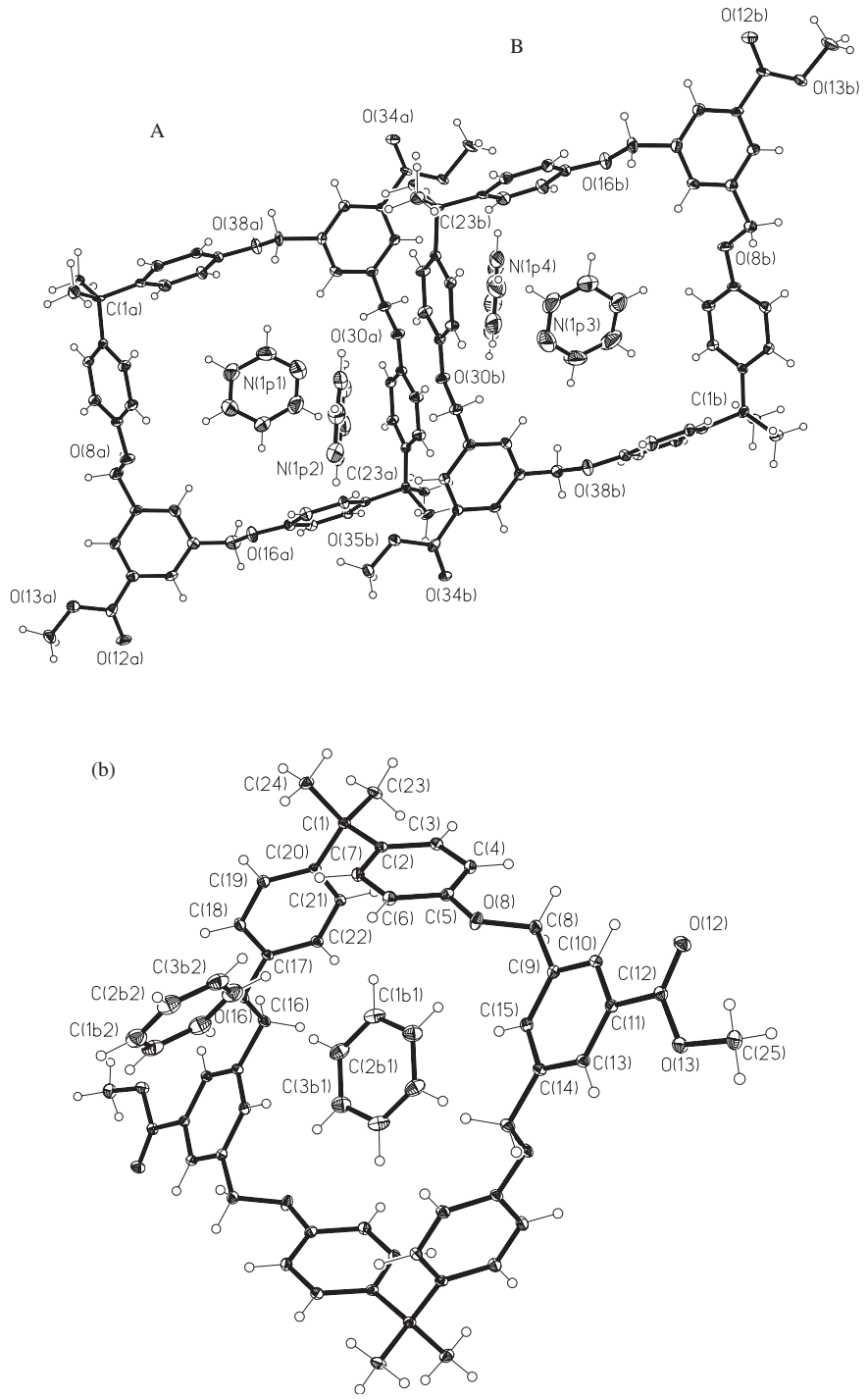


FIGURE 5 Perspective views showing the unique part of the **6a**·pyridine (1:2) co-crystal (a) and the stoichiometric entity of the **6a**·benzene (1:2) complex (b). The atomic displacement ellipsoids are drawn at 30% probability level. Selected atoms in (a) and the unique non-hydrogen atoms in (b) are labelled.

units ($Z' = 4$). Though the packing arrangement exhibits approximate inversion symmetry (pseudo-centrosymmetry) (Figs. 5a and 6), the direct method applications (SHELXS) [32] together with the least-squares (LS) refinement calculations [33] proved the enantiomorphous $P2_1$ space group symmetry ($Z = 2$) for the monoclinic cell (cf. the experimental part). Hence, two **6a** host molecules (A and B) and four pyridine guests (P1–P4) together form a crystallographic asymmetric unit of considerable size (Fig. 5a, 140 non-H atoms, 1370 independent parameters). Although three of the pyridine molecules were present already in the preliminary electron density map (calculated using preliminary phases from the direct method applications) and the fourth one could be easily deduced from a subsequent difference electron density calculation, and despite using low-temperature X-ray data

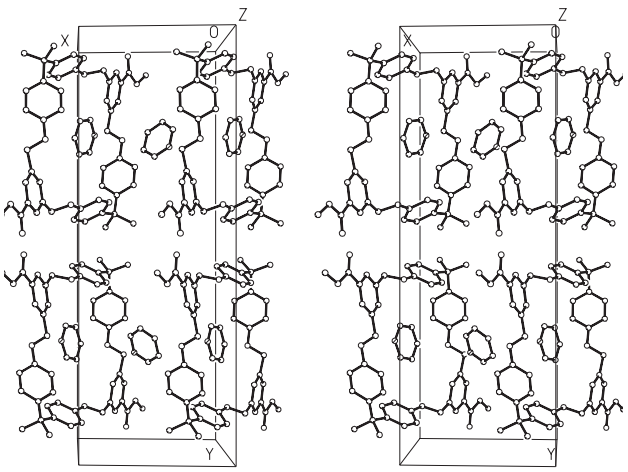


FIGURE 6 Stereo packing illustration of the **6a**·pyridine (1:2) inclusion crystal. H atoms are omitted for clarity.

(173 K, Table I), it proved difficult to determine which ring-atom in each pyridine is the hetero atom. Our observations suggest that the weakly bonded pyridines are disordered in such a way that their nitrogen atoms occupy different ring positions in different unit cells (i.e. they are statically disordered). This is a situation, which could hardly be resolved into distinct disorder sites. Therefore, the nitrogen positions in the final structure model have been selected so as to yield favourable displacement parameters for the pyridine ring atoms and, at the same time, the lowest possible crystallographic R-values for the whole structure.

On the contrary, crystals of the related **6a**·benzene (1:2) inclusion compound proved to have inversion symmetry ($P2_1/c$, $Z = 4$), and the monoclinic unit cell contains only two **6a** host molecules and four benzene guests ($Z' = 2$). Since the molecular and crystallographic inversion symmetries coincide for the host as well as the two guest molecules (B1 and B2, Fig. 5b), the unique part of the cell contains only one half of the macrocyclic **6a** and one half of each of the two benzene molecules. Consequently, the solid-state conformation of the **6a** cyclophane ester is centrosymmetric in its benzene inclusion crystal, whereas the two independent **6a** molecules (A and B, Fig. 5a) in the **6a**·pyridine (1:2) co-crystal have no crystallographic symmetry. This is also obvious from the dihedral angles formed by the aromatic moieties with opposite locations in the macrocyclic rings, i.e. rings A/A′, B/B′ and C/C′ (Schemes 1 and 2). If the cyclophane ring had crystallographic inversion symmetry, all these three dihedral angles would show zero values (indicating exact co-planarity due to the symmetry requirements). But the dihedral angles calculated for each of the three pairs of phenyl ring planes (A/A′, B/B′ and C/C′) for both independent molecules in the **6a**·pyridine (1:2) complex indicate significant deviations from co-planarity (Table II), though these latter values are considerably lower than those noted for the related asymmetric host **1** macrocycle in its **1**·DMSO (1:4) inclusion crystal.

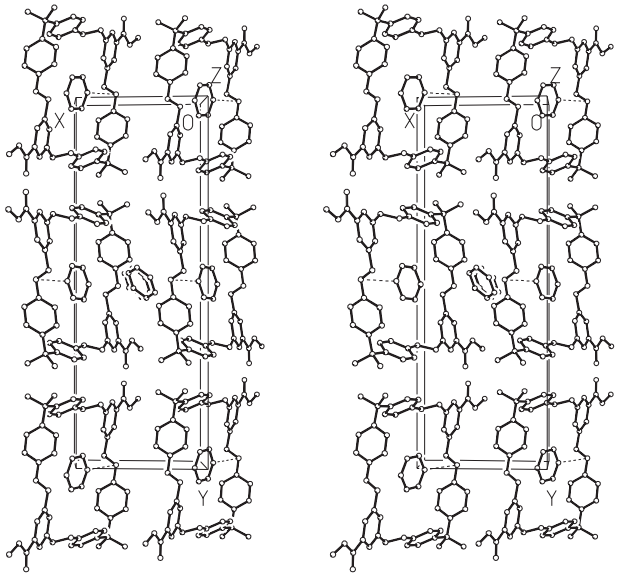


FIGURE 7 Stereo packing illustration of the **6a**·benzene (1:2) inclusion crystal. H atoms are omitted for clarity.

In the two inclusion compounds of the ester-substituted cyclophane host **6a**, the molecules pack so as to make a number of intermolecular C–H···O type approaches possible (Figs. 6 and 7). Only the most probable C–H···O bonds are listed in Table III and, as seen, they connect host macrocycles. The interactions between host and guest molecules are also of the C–H···O type, but these latter ones have somewhat longer distances (i.e. are weaker) than those between the hosts. The four shortest host–guest connections in **6a**·pyridine (1:2), one to each of the four unique P1–P4 pyridines (Fig. 5a), have C···O/H···O distances between 3.50–3.75/2.77–2.92 Å, whereas the corresponding distances involving the B1–B2 benzenes in **6a**·benzene (1:2) (Fig. 5b) are 3.53–3.86/2.89–2.96 Å. It could be a consequence of the relatively weak host–guest interaction forces that the **6a** macrocycle adopts a less strained conformation in the present inclusion crystals, in which the C($sp^2$)–C($sp^3$)–O–C($sp^2$) sequences are *anti-periplanar* (τ ranging between 162° and 170°, Table II) and the phenyl rings of each bis-phenol moiety are nearly perpendicular to each other (dihedral angles formed by the A/C′ and A′/C ring planes are between 83.7° and 87.0°, Table II).

### *Unsolvated Cyclophane Hosts*

Crystallization of the diesters **6a** and **6b** from mesitylene or *p*-xylene solvents yielded guest-free crystals with triclinic ($P\,-\,1$) and monoclinic ($P2_1/n$) space group symmetries, respectively, and with only

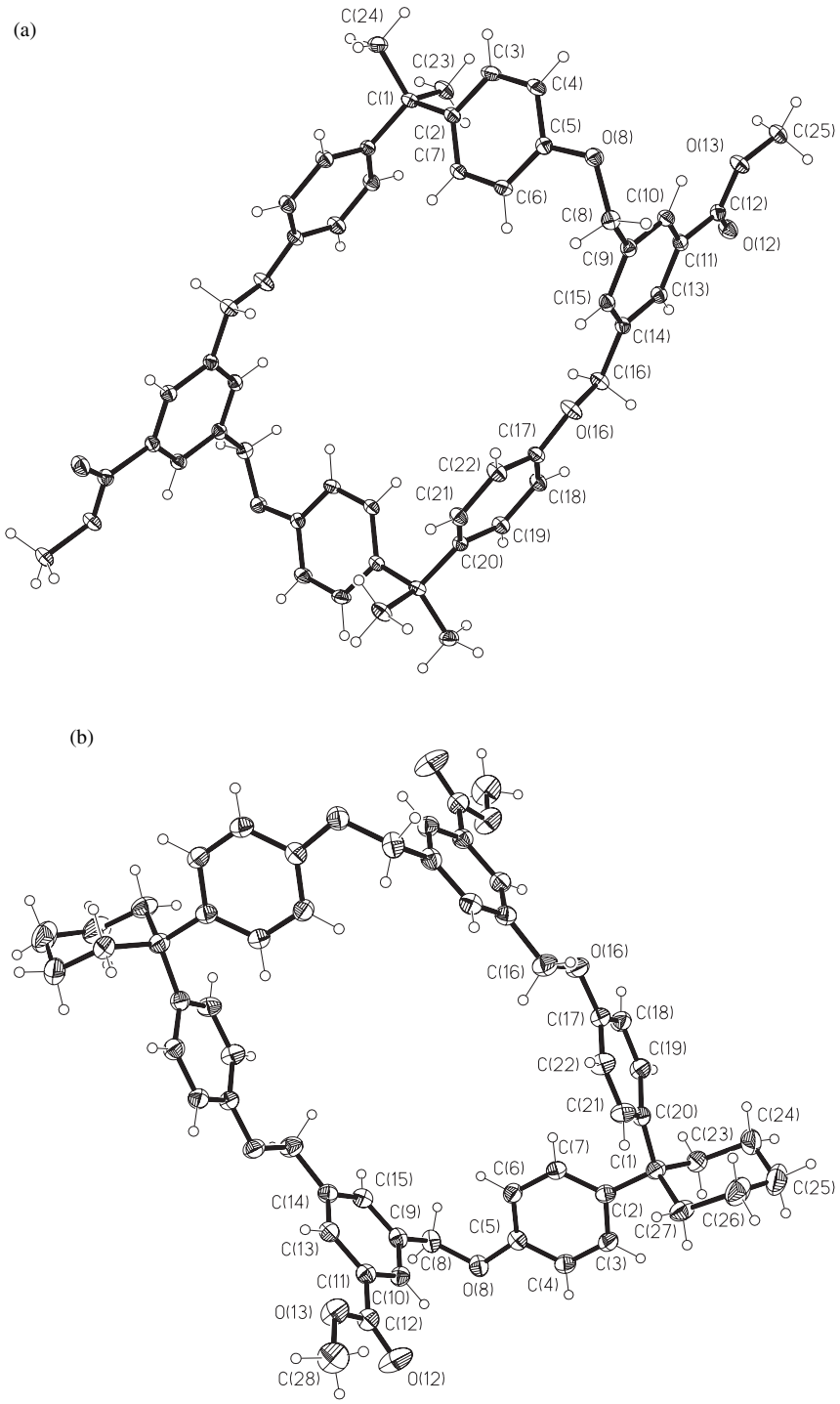


FIGURE 8 Perspective views of the unsolvated diester cyclophanes **6a** (a) and **6b** (b), with crystallographic numbering of the unique non-hydrogen atoms. The atomic displacement ellipsoids of the carbon and oxygen atoms are drawn at 30% probability level.

one half of the macrocyclic molecule in the asymmetric unit in both compounds (Fig. 8a–b). These two ester hosts in their solvent-free crystals show similar ring conformations, which, at the same time, deviate from the conformations exhibited by the **6a** molecule in its inclusion crystals, and also from those observed for the carboxylic hosts **1**, **2** and **3** (Table II). Contrary to the related macrocycles listed in Table II, the solvent-free **6a**–**6b** hosts adopt elongated shapes, in which the neighbouring B (C(9)···C(14)) and C (C(17)···C(22)) phenyl rings are roughly co-planar with each other (Scheme 2, Fig. 8a–b). The dihedral angles, formed by the B and C phenyl planes, take low values: 11.98(7) in **6a** and 22.94(7)° in **6b**. On the other hand, although these two cyclophane esters carry different substituents on the bridging carbon in their bis-phenol moieties (Scheme 2), the A/C′ ring planes are nearly

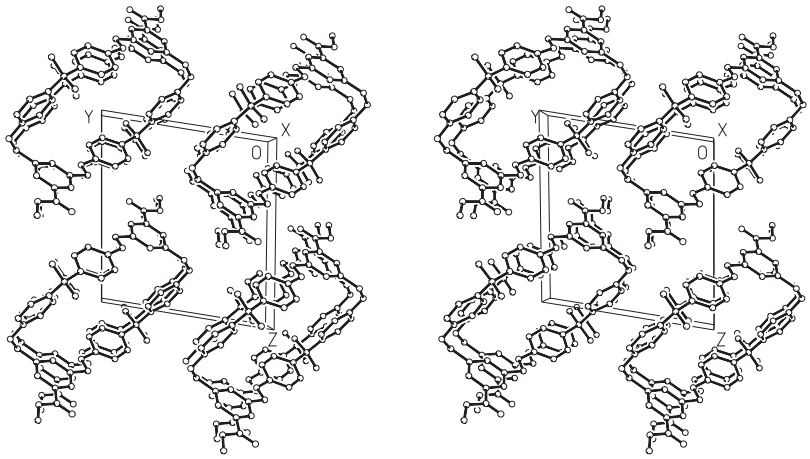


FIGURE 9 Stereo packing illustration of the unsolvated diester cyclophane **6a**. H atoms are omitted for clarity.

perpendicular to each other in both molecules (the dihedral angles are 82.71(4) in **6a**, and 88.60(5)° in **6b**), just as in most of the studied cyclophane hosts (Table II). A survey of the calculated torsion angles for the solvent-free ester structures suggests absence of ring strain. Worth noting is that the torsion angles ($\tau$) of the two unique $C(sp^2)-C(sp^3)-O-C(sp^2)$ sequences in each macrocycle yielded different values, indicating *synclinal* arrangement for the A and B phenyl rings, and *anticlinal* conformation for the linkage between the B and C rings in both guest-free host molecules.

The unsolvated cyclophane esters **6a** and **6b** were found to realize similar packing arrangements, in which the macrocyclic molecules are piled one upon the other so as to form endless parallel columns (Figs. 9 and 10). Inspection of the intermolecular distances indicates only a few possible C–H···O connections (Table III) besides the common van der Waals contacts. Accordingly, the similar packing modes may be a consequence of the fact that shape recognition has played an important role in the crystallization of both compounds, which have similar macrocyclic ring conformations.

## CONCLUSION

Three new functional cyclophanes **1**–**3**, carrying two exo-topic carboxylic groups, were prepared and shown to form crystalline inclusion compounds with polar solvents, such as DMSO and pyridine, while the corresponding ester intermediates **6** (**a**, **b**) were found to form stable crystals on their own (e.g. from mesitylene or *p*-xylene solvents), in addition to the solid inclusion compounds of **6a**, containing benzene or pyridine as guest. Accordingly, cyclophane hosts **1**–**3** exhibit inclusion selectivity by prefering guests capable for hydrogen bond formation with the host carboxy function, whereas requirement of an electrostatically favourable packing with acceptable density seems to be the most important fact in the crystal formation of the corresponding ester intermediates **6** (**a**, **b**).

Though the carboxylic group is prone to form a robust supramolecular synthon in the form of a cyclic hydrogen bonded dimer [17], the present study shows a departure from this behavior. In the crystalline complexes of **1**–**3**, the carboxylic groups exclusively contact via hydrogen bonding to solvent

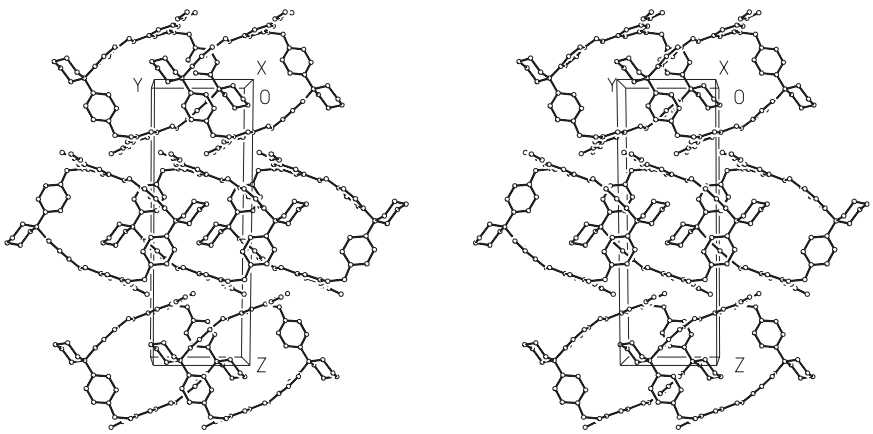


FIGURE 10 Stereo packing illustration of the unsolvated diester cyclophane **6b**. H atoms are omitted for clarity.

TABLE II Selected conformational parameters of the cyclophane macrocycles **1**, **2**, **3**, **6a** and **6b**, as observed in their crystalline inclusions and/or unsolvated compounds.

| Macrocyclic host molecule | **1** in **1**·DMSO (1:4) | **2** in **2**·Pyridine (1:3) | **3** in **3**·Pyridine (1:4) | **6a** in **6a**·Pyridine (1:2) mol. A | mol. B | **6a** in **6a**·Benzene (1:2) | **6a** (unsolvated) | **6b** (unsolvated) |
|---|---|---|---|---|---|---|---|---|
| *Selected torsion angles* (°) | | | | | | | | |
| C(5)–O(8)–C(8)–C(9) | 178.6(3) | 174.0(2) | −155.1(4) | 168.5(2) | −167.1(2) | −165.1(1) | 65.2(2) | −74.5(2) |
| C(14)–C(16)–O(16)–C(17) | 103.0(5) | −160.7(2) | −177.5(4) | −167.9(2) | −169.5(2) | 169.1(1) | 166.0(1) | −159.9(1) |
| C(27)–O(30)–C(30)–C(31) | −173.8(3) | | | 163.1(2) | −162.5(2) | | | |
| C(36)–C(38)–O(38)–C(39) | 145.1(3) | | | 165.1(2) | −166.3(2) | | | |
| *Dihedral angle between selected phenyl ring planes* (°)[a] | | | | | | | | |
| Ring A/ring B | 81.9(1) | 69.49(7) | 70.4(1) | 65.42(8) | 64.77(8) | 51.64(4) | 82.51(4) | 87.49(5) |
| Ring A′/ring B′ | 51.8(1) | | | 89.86(7) | 87.49(7) | | | |
| Ring A/ring C′ | 89.2(1) | 82.88(8) | 85.5(1) | 84.87(7) | 86.35(7) | 83.73(3) | 82.71(4) | 88.60(5) |
| Ring A′/ring C | 85.8(1) | | | 87.06(7) | 84.38(7) | | | |
| Ring B/ring C | 89.2(1) | 77.50(8) | 78.0(1) | 63.71(8) | 64.39(8) | 86.94(3) | 11.98(7) | 22.94(7) |
| Ring B′/ring C′ | 48.9(1) | | | 47.63(9) | 51.22(9) | | | |
| Ring A/ring A′ | 73.3(1) | 0.00 | 0.00 | 18.36(7) | 21.49(7) | 0.00 | 0.00 | 0.00 |
| Ring B/ring B′ | 26.21(8) | 0.00 | 0.00 | 16.72(8) | 14.48(8) | 0.00 | 0.00 | 0.00 |
| Ring C/ring C′ | 43.6(2) | 0.00 | 0.00 | 3.4(1) | 1.6(1) | 0.00 | 0.00 | 0.00 |
| *Dihedral angle between the functionalised phenyl ring plane*[a] *and the attached* −COO *plane* (°) | | | | | | | | |
| Ring B/COO | 8.2(5) | 19.8(2) | 1.8(4) | 6.1(2) | 7.5(3) | 11.67(9) | 5.7(1) | 6.9(2) |
| Ring B′/COO | 1.9(2) | | | 17.4(3) | 17.5(2) | | | |

[a] Ring A: C2···C7; ring B: C9···C14; ring C: C17···C22; ring A′: C24···C29; ring B′: C31···C36; ring C′: C39···44 (see Schemes 1 and 2).

molecules, giving rise to space for the accommodation of additional solvent molecules in true inclusion fashion [34], resulting in the remarkably high stoichiometric host:guest ratios (1:3 and 1:4, respectively). Nevertheless, considering the new type of cyclophane hosts that may allow modification of the exo-topic functions, self-assembly via the supramolecular synthon approach [35,36] to provide designed formation of supramolecular pattern [37] and open framework structures [38] or interwoven systems [39,40] having ordered recognition sites are promising aspects of this work [41].

## EXPERIMENTAL

### General

Melting points are uncorrected. $^{1}H$ and $^{13}C$ NMR spectra were recorded on a Bruker Avance DPX 400 instrument at 25°C. Chemical shifts are reported in ppm with TMS as an internal standard ($\delta = 0$ ppm). Mass spectra were determined on HP 59987A and MAT 95 XL (ESI), KRATOS-CONCEPT ($FAB^{+}$, matrix: 3-nitrobenzyl alcohol), and HP G2025A (MALDI-TOF-MS, matrix: 2,6-dihydroxybenzoic acid) instruments. The elemental analyses were performed with a Heraeus CHN rapid analyzer.

### Starting Compounds

Methyl 3,5-bis(bromomethyl)benzoate **(4)** was obtained from 3,5-dimethylbenzoic acid by esterification to the corresponding methyl ester [42] and subsequent NBS-bromination [21]. Bisphenol **5a** is commercially available (Aldrich). Bisphenols **5b** [22,23] and **5c** [23] were prepared by literature procedures.

### Synthesis of Macrocyclic Compounds 6a, 6b and 6c. General Procedure

The reactions were performed in a standardized 1-component dilution equipment [15,16,43]. Under an atmosphere of argon, cesium carbonate (13.04 g, 40 mmol) and molecular sieve (4 Å, 5 g) were suspended in dry acetone (1250 ml). The stirred suspension was heated to reflux, and a mixture of **4** (6.44 g, 20 mmol) and the corresponding bisphenol **5a–c** (20 mmol) in dry acetone (500 ml) was added dropwise during 8 h. After heating to reflux and stirring for an additional 3 h, the reaction mixture was allowed to stand overnight. The solvent was evaporated and the residue was taken up in dichloromethane and carefully filtered through silica gel. Specific details are given for each compound.

TABLE III Geometry of intermolecular O–H···O hydrogen bonds and selected C–H···O connections[a] in the studied compounds

| Atoms involved | Symmetry | Distance (Å) D···A | Distance (Å) H···A | Angle (°) D-H···A |
|---|---|---|---|---|
| **1** DMSO (1:4) | | | | |
| O(13)–H(13O)···O(1G1) | $x, y, z$ | 2.554(6) | 1.63 | 149 |
| O(13)–H(13O)···O(2G1) | $x, y, z$ | 2.686(12) | 1.69 | 166 |
| O(35)–H(35O)···O(1G2) | $x, y, z$ | 2.550(7) | 1.74 | 144 |
| O(35)–H(35O)···O(2G2) | $x, y, z$ | 2.671(8) | 1.78 | 162 |
| C(8)–H(8)···O(1G3) | $-x, 1-y, -z$ | 3.491(7) | 2.53 | 169 |
| C(30)–H(30)···O(1G4) | $-x, 1-y, 1-z$ | 3.346(6) | 2.59 | 135 |
| C(38)–H(38)···O(34) | $-1-x, -y, 1-z$ | 3.335(5) | 2.52 | 142 |
| C(1G1)–H(3G1)···O(34) | $1+x, 1+y, -1+z$ | 3.237(14) | 2.54 | 130 |
| C(41)–H(41)···O(1G2) | $-1-x, -y, 1-z$ | 3.367(8) | 2.67 | 132 |
| C(1G3)–H(2G3)···O(1G4) | $x, y, z$ | 3.193(8) | 2.54 | 125 |
| C(1G3)–H(3G3)···O(2G1) | $-x, 1-y, -z$ | 3.484(15) | 2.58 | 156 |
| C(2G3)–H(6G3)···O(1G4) | $x, y, z$ | 3.240(9) | 2.45 | 139 |
| C(2G4)–H(6G4)···O(1G3) | $1+x, y, z$ | 3.211(9) | 2.36 | 148 |
| **2**·Pyridine (1:3) | | | | |
| O(13)–H(13O)···N(1P1) | $x, y, z$ | 2.648(3) | 1.67 | 159 |
| C(13)–H(13)···O(12) | $-x, 3-y, 2-z$ | 3.392(3) | 2.56 | 149 |
| C(24)–H(24B)···O(16) | $x, 1+y, z$ | 3.467(3) | 2.80 | 126 |
| **3**·Pyridine (1:4) | | | | |
| N(1P1)–H(1P1)···O(13) | $x, y, z$ | 2.750(7) | 1.91 | 164 |
| N(1P2)···O(12) | $x, y, z$ | 2.612(8) | | |
| **6a**·Pyridine (2:4) | | | | |
| C(13A)–H(13A)···O(34°) | $x+2, y+0.5, -z+1$ | 3.396(3) | 2.70 | 125 |
| C(29A)–H(29A)···O(38B) | $x+1, y, z$ | 3.436(4) | 2.66 | 140 |
| C(35A)–H(35A)···O(34B) | $x+1, y-0.5, -z+1$ | 3.454(3) | 2.62 | 146 |
| C(45A)–H(45B)···O(16B) | $x+1, y, z+1$ | 3.435(3) | 2.67 | 136 |
| C(48A)–H(48C)···O(38B) | $x+1, y, z$ | 3.490(3) | 2.60 | 151 |
| C(29B)–H(29B)···O(38A) | $x-1, y, z$ | 3.428(3) | 2.65 | 140 |
| C(47B)–H(47E)···O(38A) | $x-1, y, z$ | 3.440(3) | 2.60 | 144 |
| C(46B)–H(46D)···O(16A) | $x-1, y, z$ | 3.425(3) | 2.62 | 139 |
| C(6P4)–H(6P4)···O(35A) | $x, y, z$ | 3.497(4) | 2.76 | 135 |
| **6a**·Benzene (1:2) | | | | |
| C(21)–H(21)···O(8) | $x, y, z-1$ | 3.433(1) | 2.64 | 141 |
| C(23)–H(23)···O(8) | $x, y, z-1$ | 3.440(1) | 2.62 | 142 |
| **6a**·(unsolvated) | | | | |
| C(8)–H(8)···O(13) | $-x+2, -y+3, -z+1$ | 3.478(2) | 2.54 | 158 |
| C(25)–H(25B)···O(8) | $-x+3, -y+3, -z+1$ | 3.424(2) | 2.78 | 124 |
| **6b**·(unsolvated) | | | | |
| C(8)–H(8)···O(12) | $-x-1.5, y-0.5, -z+0.5$ | 3.126(2) | 2.47 | 125 |

[a] The most probable C–H···O bonds with C···O distance shorter than 3.50 Å, and C–H···O angle larger than 120° were selected. Esd's, where given, are in parentheses. The H atom positions were not refined (cf. the text).



### *Dimethyl 17,17,40,40-tetramethyl-1,10,24,33-tetraoxa-[2](1,3)benzeno[2](1,4)benzeno[1](1,4)benzeno[2](1,3)benzeno[2](1,4)benzenophane-5,28-dicarboxylate (6a)*

2,2-Bis(4-hydroxyphenyl)propane (**5a**) (4.56 g, 20 mmol) was used. After removal of the solvent under reduced pressure, the raw product was taken up in benzene (150 ml) and stirred for 4 h. Filtration by suction yielded 2.0 g (26%) of white crystals; mp 249–251°C; $^1$H NMR (400 MHz, $CDCl_3$) δ 1.63 (s, 12 H, $CH_3$), 3.93 (s, 6 H, $OCH_3$), 5.09 (s, 8 H, $CH_2$), 6.79 (d, 8 H, J = 8.8 Hz, Ar–H), 7.08 (d, 8 H, J = 8.8 Hz, Ar–H), 7.64 (s, 2 H, Ar–H), 7.99 (s, 4 H, Ar–H); $^{13}$C NMR (100 MHz, $CDCl_3$) δ 30.63 ($CH_3$), 41.60 (qC), 52.26 ($OCH_3$), 69.37 ($CH_2$), 114.36 (Ar), 127.52 (Ar), 127.70 (Ar), 130.37 (Ar), 130.71 (Ar), 138.54 (Ar), 143.66 (Ar), 156.34 (Ar), 166.69 (COO); MS ($FAB^+$) $m/z$ Calcd for $C_{50}H_{48}O_8$: 776.3. Found: 776.3 ($M^+$). Anal. calcd for $C_{50}H_{48}O_8$: C, 77.30; H, 6.23. Found: C, 77.29; H, 6.26.

### *Dimethyl 1′,10′,24′,33′-tetraoxadispiro[cyclohexane-1,17′-([2](1,3)benzeno[2](1,4)benzeno[1](1,4)benzeno[2](1,3)benzeno[2](1,4)benzeno[1](1,4)benzenophane)-40′,1″-cyclohexane]-5′,28′-dicarboxylate (6b)*

1,1-Bis(4-hydroxyphenyl)cyclohexane (**5b**) (5.37 g, 20 mmol) was used. Evaporation of the solvent and recrystallization from benzene yielded 2.2 g (26%) white crystals; mp 268–270°C; $^1$H NMR (400 MHz, $CDCl_3$) δ 1.55 (m, 12 H, $CH_2$), 2.20 (s, 8 H, $CH_2$), 3.93 (s, 6 H, $OCH_3$), 5.05 (s, 8 H, $CH_2$), 6.79 (d, 8 H, J = 8.8 Hz, Ar–H), 7.11 (d, 8 H, J = 8.8 Hz, Ar–H), 7.61 (s, 2 H, Ar–H), 7.99 (s, 4 H, Ar–H); $^{13}$C NMR (100 MHz, $CDCl_3$) δ 22.93 ($CH_2$), 26.42 ($CH_2$), 37.06 ($CH_2$), 44.94 (qC), 52.25 ($OCH_3$), 69.30 ($CH_2$), 114.47 (Ar), 127.54

(Ar), 128.01 (Ar), 130.42 (Ar), 130.68 (Ar), 138.53 (Ar), 141.62 (Ar), 156.10 (Ar), 166.69 (COO); MS (MALDI-TOF) $m/z$ calcd for $C_{56}H_{56}O_8$: 856.4. Found: 880.6 ($[M + Na]^+$), 896.7 ($[M + K]^+$). Anal. calcd for $C_{56}H_{56}O_8$: C, 78.48; H, 6.59. Found: C, 78.82; H, 6.67.

***Dimethyl 12′,16′,20′,22′,35′,39′,43′,45′-octamethyl-1′,10′,24′,33′-tetraoxadispiro[cyclohexane-1,17′-([2](1,3)benzeno[2](1,4)benzeno[1](1,4)benzeno[2](1,3)benzeno[2](1,4)benzeno[1](1,4)benzenophane)-40′,1″-cyclohexane]-5′,28′-dicarboxylate (6c)***

1,1-Bis(4-hydroxy-3,5-dimethylphenyl)cyclohexane (**5c**) (6.49 g, 20 mmol) was used. After removal of the solvent under reduced pressure, the raw product was taken up in benzene (150 ml) and heated to reflux for 1 h. Filtration by suction yielded 2.1 g (22%) of white solid; mp 299–302°C; $^1$H NMR (400 MHz, $CDCl_3$) δ 1.53 (m, 12 H, $CH_2$), 2.11 (s, 24 H, $CH_3$), 2.18 (s, 8 H, $CH_2$), 3.95 (s, 6 H, $OCH_3$), 4.86 (s, 8 H, $CH_2$), 6.84 (s, 8 H, Ar–H), 7.58 (s, 2 H, Ar–H), 8.07 (s, 4 H, Ar–H); $^{13}$C NMR (100 MHz, $CDCl_3$) δ 16.91 ($CH_3$), 22.88 ($CH_2$), 26.35 ($CH_2$), 36.95 ($CH_2$), 44.88 (qC), 52.09 ($OCH_3$), 73.38 ($CH_2$), 127.40 (Ar), 128.15 (Ar), 129.81 (Ar), 130.48 (Ar), 131.36 (Ar), 138.71 (Ar), 144.01 (Ar), 153.30 (Ar), 166.75 (COO); MS (ESI) $m/z$ calcd for $C_{64}H_{72}O_8$: 968.5. Found: 991.3 ($[M + Na]^+$), 1007.2 ($[M + K]^+$). Anal. calcd for $C_{64}H_{72}O_8$: C, 79.31; H, 7.49. Found: C, 79.43; H, 7.64.

## Synthesis of Host Compounds 1, 2 and 3. General Procedure

To a suspension of the corresponding diester (**6a–c**) (1 mmol) in *n*-butanol (50 ml) was added cesium hydroxide monohydrate (3.36 g, 20 mmol) dissolved in 2 ml of water. The mixture was heated to reflux until the solid was dissolved. To complete the reaction, the solution was heated to reflux for an additional 3 h. The solvent was evaporated under reduced pressure (complete removal of *n*-butanol was achieved by co-evaporation with water and ethanol in this sequence). The solid residue was suspended in water (50 ml), acidified with hydrochloric acid (2 N) and stirred for 1 h at room temperature. The precipitate was collected, thoroughly washed with water and little cold ethanol, and dried. Specific details are given for each compound.

***17,17,40,40-Tetramethyl-1,10,24,33-tetraoxa-[2](1,3)benzeno[2](1,4)benzeno[1](1,4)benzeno[2](1,3)benzeno[2](1,4)benzeno[1](1,4)benzenophane-5,28-dicarboxylic Acid (1)***

Diester **6a** (0.78 g, 1 mmol) was used to yield 0.63 g (84%) of white solid; mp >330°C; $^1$H NMR (400 MHz, DMSO-$d_6$) δ 1.57 (s, 12 H, $CH_3$), 5.16 (s, 8 H, $CH_2$), 6.82 (d, 8 H, J = 8.8 Hz, Ar–H), 7.05 (d, 8 H, J = 8.8 Hz, Ar–H), 7.63 (s, 2 H, Ar–H), 7.92 (s, 4 H, Ar–H); $^{13}$C NMR (100 MHz, DMSO-$d_6$) δ 30.43 ($CH_3$), 41.14 (qC), 68.46 ($CH_2$), 114.31 (Ar), 127.45 (Ar, 2 signals), 130.23 (Ar), 131.51 (Ar), 138.44 (Ar), 142.98 (Ar), 155.87 (Ar), 167.13 (COO); MS (ESI) $m/z$ calcd for $C_{48}H_{44}O_8$: 748.3. Found: 747 ($[M - H^+]^-$), 373 ($[M - 2H^+]^{2-}$). Anal. calcd for $C_{48}H_{44}O_8 \cdot H_2O$: C, 75.18; H, 6.05. Found: C, 75.13; H, 6.01.

***1′,10′,24′,33′-Tetraoxadispiro[cyclohexane-1,17′-([2](1,3)benzeno[2](1,4)benzeno[1](1,4]benzeno[2](1,3)benzeno[2](1,4)benzeno[1](1,4)benzenophane)-40′,1″-cyclohexane]-5′,28′-dicarboxylic Acid (2)***

Diester **6b** (0.86 g, 1 mmol) was used to yield 0.85 g (99%) of white solid; mp >330°C; $^1$H NMR (400 MHz, DMSO-$d_6$) δ 1.44 (s, 12 H, $CH_2$), 2.17 (s, 8 H, $CH_2$), 5.11 (s, 8 H, $CH_2$), 6.81 (d, 8 H, J = 6.4 Hz, Ar–H), 7.12 (d, 8 H, J = 6.4 Hz, Ar–H), 7.59 (s, 2 H, Ar–H), 7.93 (s, 4 H, Ar–H), 13.12 (s, 2 H, COOH); $^{13}$C NMR (100 MHz, DMSO-$d_6$) δ 22.61 ($CH_2$), 25.90 ($CH_2$), 36.20 ($CH_2$), 44.40 (qC), 68.47 ($CH_2$), 114.48 (Ar), 127.53 (Ar), 127.72 (Ar), 130.19 (Ar), 131.52 (Ar), 138.53 (Ar), 141.01 (Ar), 155.68 (Ar), 167.06 (COO); MS (MALDI-TOF) $m/z$ calcd for $C_{54}H_{52}O_8$: 828.4. Found: 852.1 ($M + Na^+$), 868.5 ($M + K^+$). Anal. calcd for $C_{54}H_{52}O_8 \cdot 1.5H_2O$: C, 75.77; H, 6.48. Found: C, 75.52; H, 6.45.

***12′,16′,20′,22′,35′,39′,43′,45′-Octamethyl-1′,10′,24′,33′-tetraoxadispiro[cyclohexane-1,17′-([2](1,3)benzeno[2](1,4)benzeno[1](1,4)benzeno[2](1,3)benzeno[2](1,4)benzeno[1](1,4)benzenophane)-40′,1″-cyclohexane]-5′,28′-dicarboxylic Acid (3)***

Diester **6c** (0.97 g, 1 mmol) was used to yield 0.7 g (73%) of white solid; mp >330°C; $^1$H NMR (400 MHz, DMSO-$d_6$) δ 1.41 (s, 12 H, $CH_2$), 2.04 (s, 24 H, $CH_3$), 2.17 (s, 8 H, $CH_2$), 4.84 (s, 8 H, $CH_2$), 6.92 (s, 8 H, Ar–H), 7.46 (s, 2 H, Ar–H), 8.01 (s, 4 H, Ar–H); $^{13}$C NMR (100 MHz, DMSO-$d_6$) δ 16.58 ($CH_3$), 22.47 ($CH_2$), 25.69 ($CH_2$), 36.09 ($CH_2$), 44.20 (qC), 72.89 ($CH_2$), 126.91 (Ar), 128.29 (Ar), 129.47 (Ar), 131.13 (Ar), 131.51 (Ar), 138.40 (Ar), 143.32 (Ar), 152.92 (Ar), 167,00 (COO); MS (ESI-TOF) $m/z$ calcd for $C_{62}H_{68}O_8$: 940.5. Found: 469 ($M - 2H)^{2-}$. Anal. calcd for $C_{62}H_{68}O_8 \cdot H_2O$: C, 77.63; H, 7.36. Found: C, 77.85; H, 7.39.

## X-ray Crystallography

Crystals suitable for X-ray single-crystal investigations were obtained by slow evaporation of the solutions of the host compounds in the respective guest solvent. Intensity data from the inclusion compounds **1**·DMSO (1:4), **2**·pyridine (1:3), **3**·pyridine (1:4), and **6a**·pyridine (1:2), and from the solvent-free compound **6b**, were collected using a STOE IPDS (Imaging Plate Diffraction System) instrument equipped with a rotating anode, whereas a Bruker APEX II diffractometer was used for the **6a**·benzene (1:2) complex and for the solvent-free **6a** crystal. Data

reduction calculations included corrections for background, Lorentz and polarization effects.

Preliminary structure models were derived by application of direct methods [32] and were refined by full-matrix least squares calculation based on $F^2$ for all reflections [33]. Some of the guest non-hydrogen atom positions, and the partially occupied disorder sites in all compounds, together with the carboxyl hydrogen positions of the macrocyclic hosts **1**–**2**, were extracted from electron density maps, whereas all other hydrogen atoms and H disorder sites were included in the models in calculated positions, using geometric evidence [33]. In general, various constraints had to be applied in the refinement of the more or less disordered guest entities in order to get acceptable geometry for them. For example, in the **1**·DMSO (1:4) and the **6a**·pyridine (1:2) structures, the guest molecules with static disorder were refined with simple distance constraints, whereas in the **3**·pyridine (1:4) complex, where each unique pyridine molecule occupies at least two partly overlapping disorder sites, only the major H-bonded guest was refined with distance constraints. The ring atoms of the minor H-bonded guest, and of both the major and minor sites of the space-filling guest were fitted to ideal hexagons. Furthermore, only the major sites of the guest H atoms were included in the final structure models of compounds **1**·DMSO (1:4) and **3**·pyridine (1:4).

The **1**·DMSO (1:4) co-crystals proved to be very unstable even at low temperature. Thus, the structure was solved using X-ray data from a single crystal included in a capillary with a drop of mother liquor. The heaviest atoms in this solid inclusion crystal, i.e. the sulphur atoms of the four unique DMSO guests, proved to be heavily disordered, which made solution and refinement of the structure rather tricky. On the other hand, the limited size and quality of the **2**·pyridine and the **3**·pyridine inclusion crystals led to intensity data of modest quality for these compounds (cf. the $R_{int}$ values in Table I). Moreover, as a consequence of the extended disorder of the guest molecules and the approximate character of the disorder models (see above), the refinement calculations ended with relatively high $R$ values for **1**·DMSO (1:4) and **3**·pyridine (1:4).

The **6a**·pyridine (1:2) co-crystal proved to have a monoclinic unit cell, with the only strictly valid space group extinctions for the *0k0* reflections with odd $k$ values. The phase problem could be easily solved assuming the enantiomorphous $P2_1$ space group symmetry, yielding two macrocyclic hosts and four pyridine guest molecules in the crystallographic asymmetric unit. However, it is obvious from the atomic parameters as well as from the illustrations (Figs. 5a and 6), that the crystal structure is nearly centrosymmetric, and the possibility of inversion symmetry for the monoclinic unit cell was also hinted by the E-value statistics [32]. Careful inspection of the reflection intensities showed that the *0kl* reflections with odd $l$ values are generally weak, and also those of *h0l* with $l =$ odd, thus suggesting the presence of approximate inversion symmetry in the crystal. Nevertheless, the calculations seem to prove the monoclinic enantiomorphous ($P2_1$) space group. Accordingly, all attempts to solve the structure assuming crystallographic inversion symmetry for the monoclinic cell failed, and so did also all the efforts to refine the structure, after suitable transformation or translation, using centrosymmetric space group symmetries. Instead, the structure could be solved applying the triclinic $P-1$ symmetry. However, at each stage of the refinement calculations [33] the yielded $R$-values were considerably higher for the triclinic ($P-1$) model than those received for the monoclinic ($P2_1$) one, although the size of the crystallographic asymmetric unit (140 unique non-hydrogen atoms) is the same in both cases. At the same time, despite of the pseudo centrosymmetry of the monoclinic unit cell, no correlation coefficients larger than 0.50 were detected in the LS refinement of the 1370 independent parameters, assuming the $P2_1$ space group symmetry. Moreover, examination of the final (monoclinic) model using the program PLATON [44] indicated no need of additional symmetry. Hence, the structure model with the monoclinic enantiomorphous $P2_1$ space group symmetry was accepted as the final, most probable one (Figs. 5a and 6). However, as a consequence of the pseudo inversion symmetry, the calculations yielded significant uncertainty for the refined Flack asymmetry parameter ($x = 0.05(1.1)$) [45], so that the handedness of the **6a**·pyridine (1:2) co-crystal could not be determined reliably.

Crystal data, experimental parameters and details of the refinement calculations are summarized in Table I. Crystallographic data for the seven investigated crystal structures have been deposited with the Cambridge Crystallographic Data Centre as supplementary publication numbers CCDC 286512 to CCDC 286518. Copies of the data can be obtained, free of charge, on application to CCDC, 12 Union Road, Cambridge CB2 1EZ, UK (Fax: +44-1223-336033, E-mail: deposit@ccdc.cam.ac.uk).

### *Acknowledgements*

This work was financially supported by the Deutsche Forschungsgemeinschaft (GRK 208, FOR 335) and the Fonds der Chemischen Industrie.

### *References*

[1] Dietrich, B.; Viout, P.; Lehn, J. -M. *Macrocyclic Chemistry*; VCH: Weinheim, 1993.
[2] Steed, J. W.; Atwood, J. L. *Supramolecular Chemistry*; Wiley: Chichester, 2000.
[3] Schneider, H. -J.; Yatsimirsky, A. *Principles and Methods in Supramolecular Chemistry*; Wiley: Chichester, 2000.

[4] Gokel, G. W. *Crown Ethers and Cryptands, Monographs in Supramolecular Chemistry*; The Royal Society of Chemistry: Cambridge, 1991; Vol. 3.
[5] Patai, S., Rappoport, Z., Eds.; *Crown Ethers and Analogs*; Wiley: Chichester, 1989.
[6] Diederich, F. *Cyclophanes, Monographs in Supramolecular Chemistry*; The Royal Society of Chemistry: Cambridge, 1991; Vol. 2.
[7] Weber, E. In *Encyclopedia of Supramolecular Chemistry*; Atwood, J. L., Steed, J., Eds.; Marcel Dekker: New York, 2003; pp 261–273.
[8] Weber, E. In *Kirk-Othmer Encyclopedia of Chemical Technology*; Kroschwitz, J. I., Ed.;, 4th ed. Wiley: New York, 1995; Vol. 14, pp 122–154.
[9] Weber, E.; Vögtle, F. In *Comprehensive Supramolecular Chemistry*; Vögtle, F., Ed.; Elsevier: Oxford, 1996; Vol. 2, pp 1–28.
[10] Diederich, F. *Angew. Chem.* **1988**, *100*, 372.
[11] Diederich, F. *Angew. Chem. Int. Ed. Engl.* **1988**, *27*, 362.
[12] Apel, S.; Lennartz, M.; Nassimbeni, L. R.; Weber, E. *Chem. Eur. J.* **2002**, *8*, 3678.
[13] Cort, A. D.; Nissinen, M.; Mancinetti, D.; Mandolini, L.; Pasquini, C.; Rissanen, K. *Supramol. Chem.* **2004**, *16*, 59.
[14] Pollex, R.; Weber, E.; Czugler, M. In *Molecular Recognition and Inclusion*; Coleman, A. W., Ed.; Kluwer: Dordrecht, 1998; pp 467–470.
[15] Weber, E.; Haase, R.; Pollex, R.; Czugler, M. *J. Prakt. Chem.* **1999**, *341*, 274.
[16] Weber, E.; Helbig, C.; Seichter, W.; Czugler, M. *J. Incl. Phenom.* **2002**, *43*, 239.
[17] Nangia, A.; Desiraju, G. R. In *Design of Organic Solids, Topics in Current Chemistry*; Weber, E., Ed.; Springer-Verlag: Berlin-Heidelberg, 1998; Vol. 198, pp 57–95.
[18] Desiraju, G. R. *Nature* **2001**, *412*, 397.
[19] Fujita, M., Ed.; *Molecular Self-Assembly—Organic Versus Inorganic Approaches, Structure and Bonding*; Springer-Verlag: Berlin-Heidelberg, 2000; Vol. 96.
[20] Kalsani, V.; Ammon, H.; Jäckel, F.; Rabe, J. P.; Schmittel, M. *Chem. Eur. J.* **2004**, *10*, 5481.
[21] Staab, H. A.; Kirrstetter, R. G. H. *Liebigs Ann. Chem.* **1979**, 886.
[22] v. Braun, J.; Anton, E.; Haensel, W.; Werner, G. *Liebigs Ann. Chem.* **1929**, *472*(1).
[23] Niederl, J. B.; Niederl, V.; Charney, J. *J. Am. Chem. Soc.* **1940**, *62*, 322.
[24] Rossa, L.; Vögtle, F. In *Cyclophanes I, Topics in Current Chemistry*; Vögtle, F., Ed.; Springer-Verlag: Berlin-Heidelberg, 1983; Vol. 113, pp 1–86.
[25] Knops, P.; Sendhoff, N.; Mekelburger, H. -B.; Vögtle, F. In *Macrocycles, Topics in Current Chemistry*; Weber, E., Vögtle, F., Eds.; Springer-Verlag: Berlin-Heidelberg, 1992; Vol. 161, pp 1–36.
[26] Ostrowicki, A.; Koepp, E.; Vögtle, F. In *Macrocycles, Topics in Current Chemistry*; Weber, E., Vögtle, F., Eds.; Springer-Verlag: Berlin, 1992; Vol. 161, pp 37–67.
[27] Csöregh, I.; Gallardo, O.; Weber, E.; Pollex, R.; Dörpinghaus, N. *J. Incl. Phenom.* **1995**, *20*, 235.
[28] Csöregh, I.; Czugler, M.; Ertan, A.; Weber, E.; Ahrendt, J. *J. Incl. Phenom.* **1990**, *8*, 275.
[29] Desiraju, G. R.; Steiner, T. *The Weak Hydrogen Bond, IUCr Monographs on Crystallography*; Oxford University Press: Oxford, 1999; Vol. 9.
[30] Meyer, E. A.; Castellano, R. K.; Diederich, F. *Angew. Chem.* **2003**, *115*, 1244.
[31] Meyer, E. A.; Castellano, R. K.; Diederich, F. *Angew. Chem. Int. Ed.* **2003**, *42*, 1210.
[32] Sheldrick, G. M. *SHELXS-97: Program for Crystal Structure Solution*; University of Göttingen: Göttingen, Germany, 1990.
[33] Sheldrick, G. M. *SHELXL-97: Program for Crystal Structure Refinement*; University of Göttingen: Göttingen, Germany, 1997.
[34] Weber, E. In *Comprehensive Supramoleculr Chemistry*; MacNicol, D. D., Toda, F., Bishop, R., Eds.; Elsevier: Oxford, 1996; Vol. 6, pp 535–592.
[35] Desiraju, G. R. *Angew. Chem.* **1995**, *107*, 2541.
[36] Desiraju, G. R. *Angew. Chem. Int. Ed.* **1995**, *34*, 2311.
[37] Whitesell, J. K., Ed.; *Organised Molecular Assemblies in the Solid State, The Molecular Solid State*; Wiley: Chichester, 1999; Vol. 2.
[38] Hertzsch, T.; Hulliger, J.; Weber, E.; Sozzani, P. In *Encyclopedia of Supramolecular Chemistry*; Atwood, J. L., Steed, J., Eds.; Marcel Dekker: New York, 2003; pp 996–1005.
[39] Philip, D.; Stoddart, J. F. *Angew. Chem.* **1996**, *108*, 1242.
[40] Philip, D.; Stoddart, J. F. *Angew. Chem. Int. Ed.* **1996**, *35*, 1154.
[41] Weber, E., Ed.; *Design of Organic Solids, Topics in Current Chemistry*; Springer-Verlag: Berlin-Heidelberg, 1998; Vol. 198.
[42] Grysziewicz-Trochimovski, M. M. E.; Schmidt, W.; Gryszie-wicz-Trochimovski, O. *Bull. Soc. Chim. Fr.* **1948**, 593.
[43] Vögtle, F. *Chemiker-Ztg*. **1972**, *96*, 396.
[44] Spek, A. L. *PLATON: A Multi Purpose Crystallographic Tool (Version 111 203)*, 1980–2003.